



De Leeuw, L. W., Martin, G., Milewski, H., Dietz, M., & Diambra, A. (2020). Polypropylene pipe interface strength on marine sandy soils with varying coarse fraction. *Proceedings of the ICE - Geotechnical Engineering*. <https://doi.org/10.1680/jgeen.19.00137>

Peer reviewed version

Link to published version (if available):
[10.1680/jgeen.19.00137](https://doi.org/10.1680/jgeen.19.00137)

[Link to publication record in Explore Bristol Research](#)
PDF-document

This is the author accepted manuscript (AAM). The final published version (version of record) is available online via Thomas Telford (ICE Publishing) at <https://www.icevirtuallibrary.com/doi/abs/10.1680/jgeen.19.00137> . Please refer to any applicable terms of use of the publisher.

University of Bristol - Explore Bristol Research

General rights

This document is made available in accordance with publisher policies. Please cite only the published version using the reference above. Full terms of use are available:
<http://www.bristol.ac.uk/red/research-policy/pure/user-guides/ebr-terms/>

Polypropylene pipe interface strength on marine sandy soils with varying coarse fraction

Author 1

- Lawrence W de Leeuw, BSc (Hons), MSc
- Department of Civil Engineering, University of Bristol, Bristol, UK
- [0000-0001-9874-7978](https://orcid.org/0000-0001-9874-7978)

Author 2

- Gary Martin, BSc (Hons)
- Department of Civil Engineering, University of Bristol, Bristol, UK

Author 3

- Henry Milewski, MEng (Hons)
- TechnipFMC, Westhill, Aberdeenshire, UK

Author 4

- Matthew S Dietz, BEng, PhD
- Department of Civil Engineering, University of Bristol, Bristol, UK
- [0000-0002-1914-1060](https://orcid.org/0000-0002-1914-1060)

Author 5

- Andrea Diambra, MEng, PhD
- Department of Civil Engineering, University of Bristol, Bristol, UK
- [0000-0003-4618-8195](https://orcid.org/0000-0003-4618-8195)

Corresponding author: Lawrence W de Leeuw

Queen's Building
Dept. Civil Engineering, University of Bristol
University Walk
Bristol
BS8 1TR
lawrence.deleeuw@bristol.ac.uk
+44 (0) 7780875046

Manuscript written 06/06/2019

Manuscript revised 09/12/2019

Words in main text: ~4750

Number of figures: 15

Number of tables: 4

Abstract

The interface shear strength of polypropylene pipeline coatings and marine sandy soils has been investigated through direct and surface-over-soil interface shear box testing. Polypropylene specimens were acquired by removal from existing manufactured steel pipes and test soils were fabricated to closely resemble typical compositions and particle size distributions of North Sea marine sediments. Test sands varied according to their coarse particle fractions, with 0%, 15% and 35% being retained on a 0.4 mm sieve. Testing was carried out at the very low stresses pertinent to pipeline interfaces between 2.5 kPa and 37.5 kPa in both loose and dense states. The experimental results suggest a dependency of the interface shear strength on the stress level and relative density with the coarse particle fraction playing a modest role. Surface characterisation and lack of volumetric deformation suggests that the shearing kinematic is predominantly grain sliding rather than rolling. Interface efficiency was largely constant despite some scatter due to variability in surface specimens. The distinct seams apparent on some of the polypropylene surfaces as inherent manufacturing artefacts had a negligible influence on interface strength. The relationship between interface strength, normalised roughness, and Shore D hardness is discussed and compared with results from other authors.

Keywords

Laboratory tests; Pipes & pipelines; Offshore engineering

1. Introduction

Subsea pipelines can either be laid directly on the seabed or, for protection against hydrodynamic loading, shielding against fishing gear, and/or increased lateral stability, buried in shallow trenches. The longitudinal and lateral forces that such systems convey are strongly influenced by the interactions that occur between the surface of the pipeline and the supporting sediments. Robust prediction of the pipeline response under various load cases is dependent on the availability of reliable estimates of the pipe-soil interface shear strength. Forces generated in the pipeline by thermal expansion and contraction may result in lateral buckling motions (Hobbs, 1984; Perinet and Simon, 2011) or axial walking phenomena (Tornes *et al.*, 2000; Carr *et al.*, 2003) which are resisted in large part by the pipe-soil interface strength (Cathie *et al.*, 2005; Bruton *et al.*, 2008). The focus of the present research is on axial motion due to pipe walking or at buckle feed-in zones.

Pipelines are commonly protected from corrosion, abrasion, and impact damage using a polypropylene coating system. While considerable experimental work has been directed toward the assessment of the interface shear strength between sand and other polymers (medium- and high- density polyethylene, PVC, epoxy, and plexiglass (e.g. Ingold, 1982; Saxena and Wong, 1984; Negussey *et al.*, 1989; O'Rourke *et al.*, 1990) little information is available for interfaces comprising the polypropylene surfaces of relevance to subsea pipelines. Furthermore, while soil grading and uniformity has been found to have little influence on the response of smooth steel surfaces (Han *et al.* 2018), there is a paucity of information for softer polymeric interfaces given variations in grading typical of marine sediments.

As a result, there is limited published industry guidance on the interface friction coefficient for subsea pipelines placed on granular seabed. Verley and Sotberg (1994) suggests an interface friction factor of 0.6 for pipelines on sandy seafloors. Current design guidance published by DNVGL (2017a; 2017b) recommends only an interface coefficient of 0.6 when computing the frictional component of the lateral resistance for sand-concrete pipeline interfaces, irrespective of other variables. It is normal practice for individual pipeline projects to acquire sufficient and adequate data for the soils on site for proper pipeline design. However, to the authors knowledge,

there does not exist a reference body of polymer pipe coating interface strength information in the published literature. The current research aims at beginning to fill this knowledge gap by improving the fundamental understanding of smooth pipe coating interface behaviour and providing some tangible experimental evidence and guidance for the selection of the interface frictional coefficient between polypropylene pipeline coating and marine sands characterised by a range of particle size distributions typical of the North Sea environment.

Herein, a series of sand-polypropylene direct shear interface tests are reported. Tests were conducted using the Winged Direct Shear Apparatus (Lings and Dietz, 2004) on fine/medium sandy soils with varying coarse material fractions. To reproduce the pertinent conditions in the field, the normal stress level ranged from 40 kPa (O'Rourke *et al.*, 1990) to 2.5 kPa (White and Cathie, 2011). Tests were conducted in a water-saturated conditions using a specially adapted interface load pad to adopt a surface-over-soil testing configuration whilst minimising sample disturbance and pre-shearing. Particular attention will be given to the characterisation and influence of surface properties like topography and its evolution through shearing, manufacturing artefacts (surface seams), and surface hardness.

2. Materials

2.1 Test soils

Particle size distributions of marine sediments from across the North Sea show considerable scatter in granulometry. To investigate the effect of granulometry variation on the interface shear strength of polypropylene coatings and seabed sediments, three granular soils of varying coarse fractions were employed. The particle size distribution of the three soils (named S0, S15, and S35 to represent the presence of 0%, 15%, and 35% of material retained by 0.40 mm aperture sieve) are reported in Figure 1 and index characteristics are presented in Table 1. Particle size distribution was determined according to BS1377-2:1990. The granular selection S0 represents a uniform fine/medium sand (coefficient of uniformity $C_u = 2.69$ and average particle size $D_{50} = 0.249\text{mm}$) characterised by the absence of any coarse particles (defined here as material retained by 0.40 mm aperture sieve). This distribution plots on the finer side of the grey shaded area in Figure 1, which represents the typical spread of distribution of North Sea sandy soils as reported

by Milewski *et al.* (2019). The other two granular selections (S15 and S35) represent a similar fine/medium sandy seafloor with the presence of coarser particles similar to as may be found in practice. The three granular soils were fabricated by sieving and mixing silica sands dredged from the Belgian coast, coarser material from the Norfolk coastline (East Lowestoft Cargo) in the North Sea, and some silica silt, in the appropriate proportions. Grains of both dredged test sands are typically subrounded to subangular.

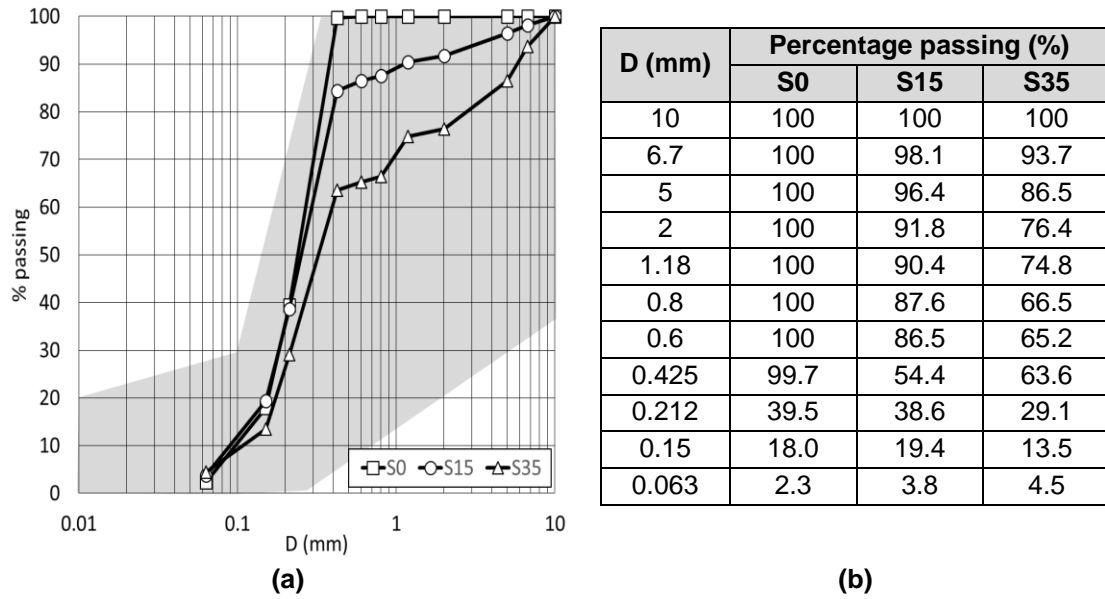


Figure 1 (a) Particle size distribution of the three materials and typical spread of particle size distribution for North Sea sediments (grey zone) after Milewski *et al.* 2019, (b) numerical values of the particle size distributions for the three materials.

Table 1 Index characteristics of the three granular soil mixtures

| | S0 | S15 | S35 |
|------------------------------------|-------|-------|-------|
| $\gamma_{max} (\text{Mg/m}^3)$ | 1.558 | 1.686 | 1.806 |
| $\gamma_{min} (\text{Mg/m}^3)$ | 1.394 | 1.505 | 1.616 |
| e_{max} | 0.901 | 0.761 | 0.640 |
| e_{min} | 0.701 | 0.572 | 0.467 |
| $D_{50} (\text{mm})$ | 0.249 | 0.265 | 0.341 |
| $C_u = D_{60} / D_{10}$ | 2.69 | 3.19 | 3.47 |
| $C_g = D_{30}^2 / (D_{10} D_{60})$ | 1.13 | 1.12 | 0.99 |

2.2 Polypropylene surfaces

Polypropylene test specimens were obtained by removal of surface coatings from already-manufactured steel pipes. Surface coatings were prised from the pipe and prepared by heating

to 160°C, flattening under load, allowing to cool to ambient temperature, still under load, before cutting to size. Examples of typical specimens are shown in Figure 2.

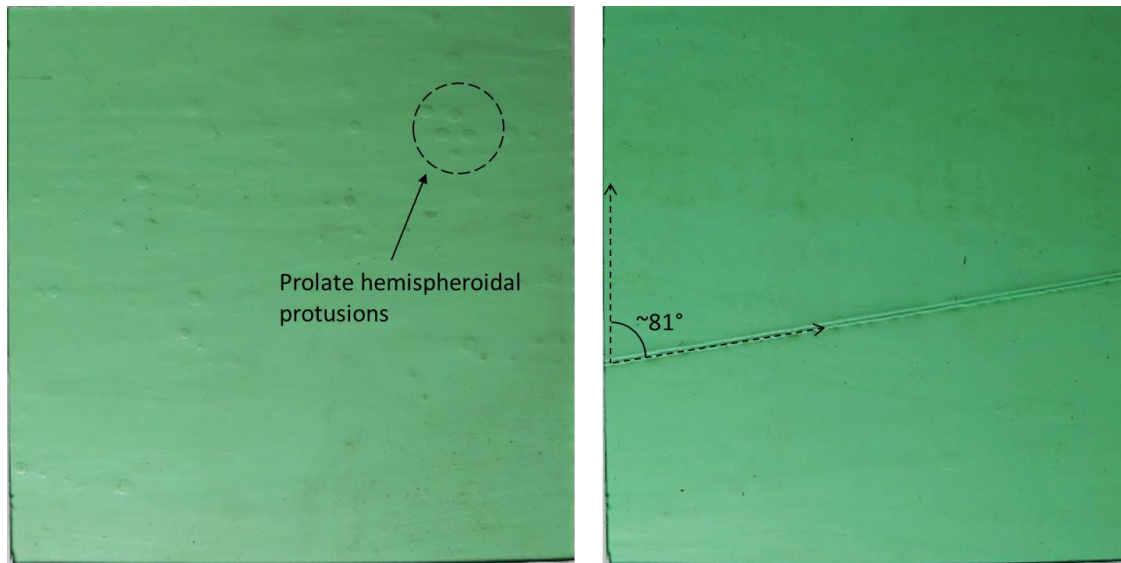


Figure 2 Photos of the polypropylene surfaces: (a) without seam (PP011) and (b) with seam (PP021).

Some of the surface specimens feature a seam across their face, artefacts of manufacturing associated with the finite width of polypropylene extrusion as it wraps around the pipe. Where present, the surface seams run at 81° to the direction of shearing. No test specimen is inscribed with more than a single seam. Other manufacturing artefacts include prolate hemispheroidal protrusions up to few millimetres across present on many of the specimens, although the number, position, and clustering of such features varies considerably. There are also other signs of imperfection such as subtle undulations and indentation which are the result of handling and transportation to the test house. Such features are common for polypropylene pipeline coatings.

2.3 Surface roughness

The roughness of the surface specimens was measured using a Taylor Hobson Form Talysurf 50 profilometer. The stylus of the instrument is a 2 µm conical diamond applying a contact force of less than 1 mN. The stylus was first lowered onto the surface specimen and then translated horizontally over a traverse length of 50 mm. Every 0.50 µm the vertical position of the stylus was digitised to produce a surface profile.

Surface texture was analysed using a 20 mm spaced orthogonal grid of ten surface profiles across the central portion of the specimen. Five profiles were measured parallel to the direction of shear (in the X direction) and five were measured perpendicular to direction of shear (in the Y direction). For each specimen, profile sets were measured both before and after testing. The schedule of profilometry is presented schematically in Figure 3.

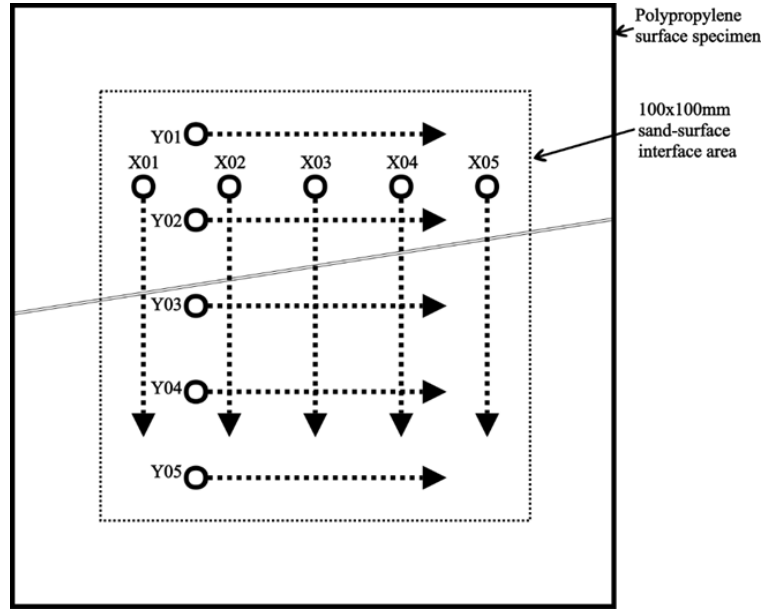


Figure 3 Schedule of profilometry across each surface specimen.

2.4 Topography characterisation

The parameter used to quantify the magnitude of the surface roughness reflected in the profiles was the arithmetic mean of absolute deviations of the profiles from their centre lines, R_a . With profile length L , and vertical deviations of a profile from its central $Z(x)$, R_a can be evaluated as:

$$R_a = \left(\frac{1}{L}\right) \int_0^L |Z(x)| dx \quad (3)$$

Following Uesugi and Kishida (1986) who recognised that there exist specific scales of interaction relevant to the contact phenomena between a granular material and a solid surface, the 50 mm long profiles were subdivided into 250 gauge lengths of 0.284 mm each, the mean D_{50} value for the three mixes of granular material under test. In each horizontal direction (X and Y) the R_a values evaluated for each of the sub-profiles were averaged to produce a representative value for the surface. $Z(x)$ is the profile height function. Figure 4 gives a schematic depiction of a surface

profile indicating R_a and another common metric, R_{max} . R_{max} is the amplitude of the largest individual combined deviation from a profile's centre line. R_a is calculated by inverting the deviations below the centre line and calculating the average absolute departure from what has now become the base line.

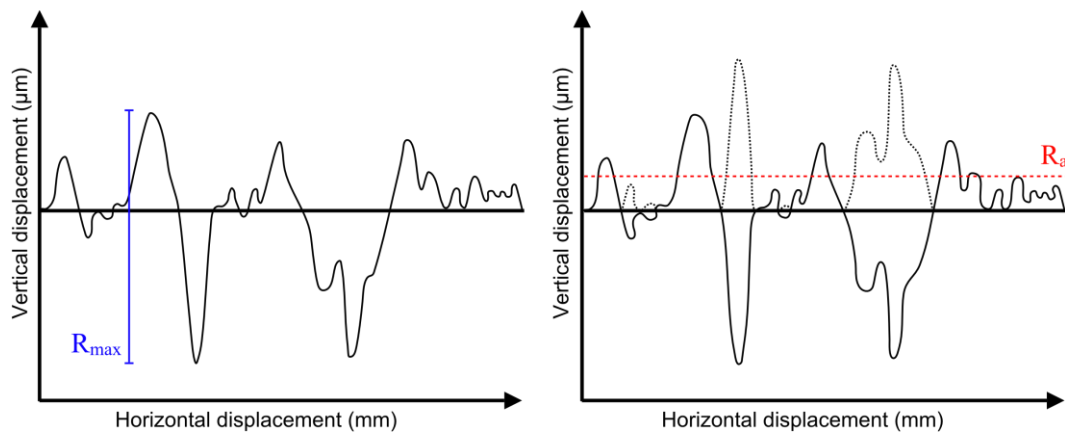


Figure 4 Schematic example of R_a and R_{max} parameters.

Quantified roughness parameters, averaged from all measurements per given surface, are presented in Figure 5 for both the X and Y directions in both pre-test (crosses) and post-test (pluses) condition. Post-test data relates to surfaces that have been subjected to a single interface test of approximately 12 mm horizontal displacement.

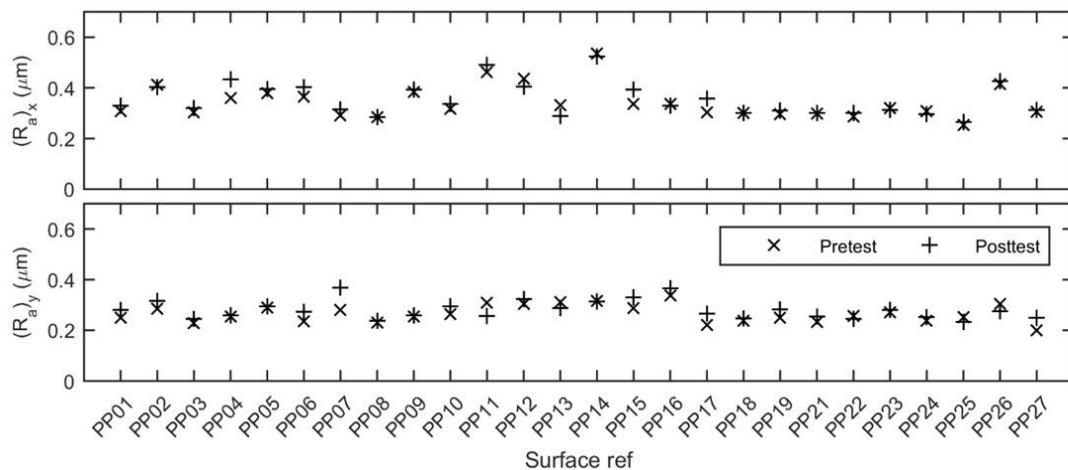


Figure 5 Quantified roughness parameters.

Surface specimen roughness exhibits a significant level of roughness variability. In the pre-test condition the coefficient of variation (i.e. the ratio of the standard deviation to the mean) for a given specimen is typically 11% in the X direction and 13% in the Y direction. Moreover, across

the entire group of twenty-six specimens, the coefficient of variation is 19% in the X direction and 13% in the Y direction. There is a greater variability of surface roughness across the group than there is on any one specimen – the full heterogeneity inherent in the topography is not represented on individual 100 mm by 100 mm surface specimens.

3. Testing Apparatus

Tests were carried out in the Winged Direct Shear Apparatus (WDSA) (Lings and Dietz, 2004), which provides an improved articulation of the force transmission compared to the conventional Direct Shear Apparatus (DSA). A schematic is presented in Figure 6 detailing its salient features and the positions of instrumentation. A pair of wings is attached to the sides of the upper frame through which the shear load is applied via ball races. The point of application of the load from shearbox to load cell is now near the centre of the sample. Parasitic forces and moments are prevented, and dilation can occur unimpeded. When conducting direct shear tests Jewell and Wroth's (1987) symmetrical arrangement was adopted to help reduce rotations by securing the load pad to the upper frame. The WDSA retains the simplicity of the conventional DSA but is much better able to reliably quantify shear forces at very low normal stress. The apparatus can accommodate a shearbox soil sample of 100 mm by 100 mm in plan dimension and approximately 50 mm high. The reliability of this apparatus was comprehensively tested and confirmed during its development by Lings and Dietz (2004) and has been used extensively in the literature for both soil and interface investigations e.g. Ibraim and Fourmont (2007) and de Leeuw et al. (2019).

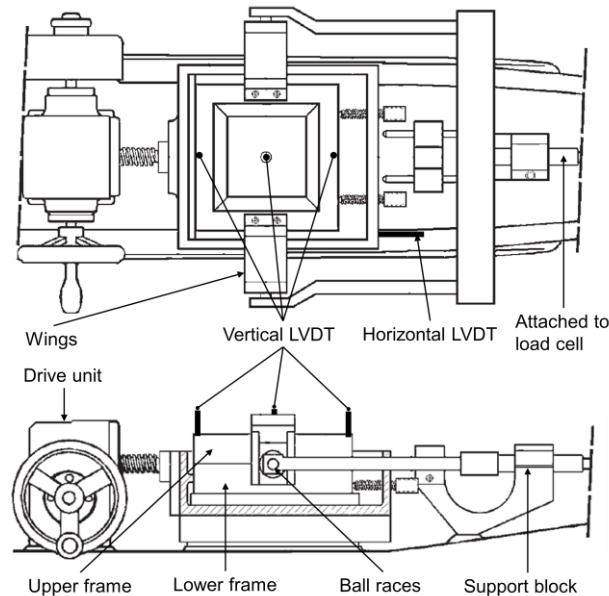


Figure 6 Schematic of the Winged Direct Shear Apparatus after Lings and Dietz (2004) including the positions of instrumentation.

The WDSA was instrumented with four Linear Variable Differential Transformers (LVDTs) measuring horizontal displacement of the carriage, vertical displacement in the centre, and vertical displacement above the leading and trailing edge of the sample. An S-Type 500 N load cell was used to measure the horizontal force required to restrain the upper portion of the apparatus during lower half translation.

3.1 Interface testing configuration

For interface tests the upper frame of the WDSA was replaced with an aluminium load pad to which surface specimens were secured with a comprehensive arrangement of countersunk perimetral bolts. Interface tests were carried out in the surface-over-soil configuration to better simulate the real conditions of a pipe lying on the seabed. Interface test configuration - surface-over-soil or soil-over-surface - has significant influence over the test results and nature of shear response. Most interface testing in the literature has been carried out in a soil-over-surface configuration where stress responses have included peak and post-peak behaviour with a dependency on surface roughness (e.g. Jardine *et al.* 1993; Subba Rao *et al.* 1998; Porcino *et al.* 2003, Lings and Dietz, 2005; Dietz and Lings, 2006). Some surface-over-soil work has been carried out in ring torsion and direct shear apparatus on metal-soil interfaces which reported only ultimate state strengths (e.g. Yoshimi and Kishida, 1981; Noornay, 1985). O'Rourke *et al.* (1990)

found that polymer-sand interface tests in a soil-over-surface configuration had a dependency of interface strength on both hardness and density, contrary to the finding of authors working with metal-soil interfaces. Subba Rao *et al.* (1998) noted that the maximum strength from surface-over-soil interface tests was analogous to the ultimate strength of soil-over-surface tests for which Uesugi and Kishida (1986) provided an explanation; placing a surface onto the soil sample disturbs the upper layers of grains, forcing them to pre-shear and rearrange to accommodate the surface texture. The adopted sample preparation methodology for interface tests in this work, described later, played a crucial role in reconciling the surface-over-soil configuration (representing typical field conditions of a pipeline on the seabed) with maintaining the best possible quality of test samples. The general message from the literature seems to be that ultimate strengths are analogous for both configurations but that only soil-over-surface tests are able to fully mobilise peak strengths because the interface zone remains undisturbed before testing.

4. Sample Fabrication

4.1 Direct shear soil tests

Soil samples for both direct shear and interface tests were prepared using the dry deposition method detailed in Miura *et al.* (1997) to achieve the maximum void ratio of a granular material. The shearbox halves were prepared with a pre-set gap between them of 1.5 mm and sand gently poured in with a funnel - ensuring zero drop height - to form a conical heap. To prevent extrusion of soil through the gap during preparation and testing, 1 mm thick strips of rubber were adhered to the internal faces of the shearbox frames prior to deposition to form a curtain to retain the soil. Use of rubber edging follows the precedent of Al-Douri and Poulos (1992) and Shibuya *et al.* (1997) who considered the effect of it on measured forces to be negligible. The top of the soil heap was then removed, and the remaining soil gently spread to achieve a flat upper surface. The load pad was placed and gently vibrated until a target sample height is achieved corresponding to the required density.

4.2 Soil-polypropylene interface tests

Interface tests were carried out in the surface-over-soil configuration to reflect seafloor conditions. This arrangement better represents real-world application and simulates a pipe lying directly on the seabed. The utilised interface preparation technique was devised to ensure repeatability of testing, to generate high quality results, and to enhance confidence that the test was effectively measuring the interface strength. Particular attention was paid to maximising the contact homogeneity between soil and surface, the uniformity of soil density throughout the sample, the prevention of any inadvertent disruption to the as-prepared interface prior to testing, and the minimising of sample extrusion during preparation and testing. To address these requirements interface samples were prepared upside down in a soil-over-surface arrangement in the same manner as soil-only direct shear tests. Once prepared, the whole assembly was secured and then smoothly but decisively inverted to the surface-over-soil orientation for placement in the shear carriage. Figure 7 is a schematic showing the stages of interface test sample preparation.

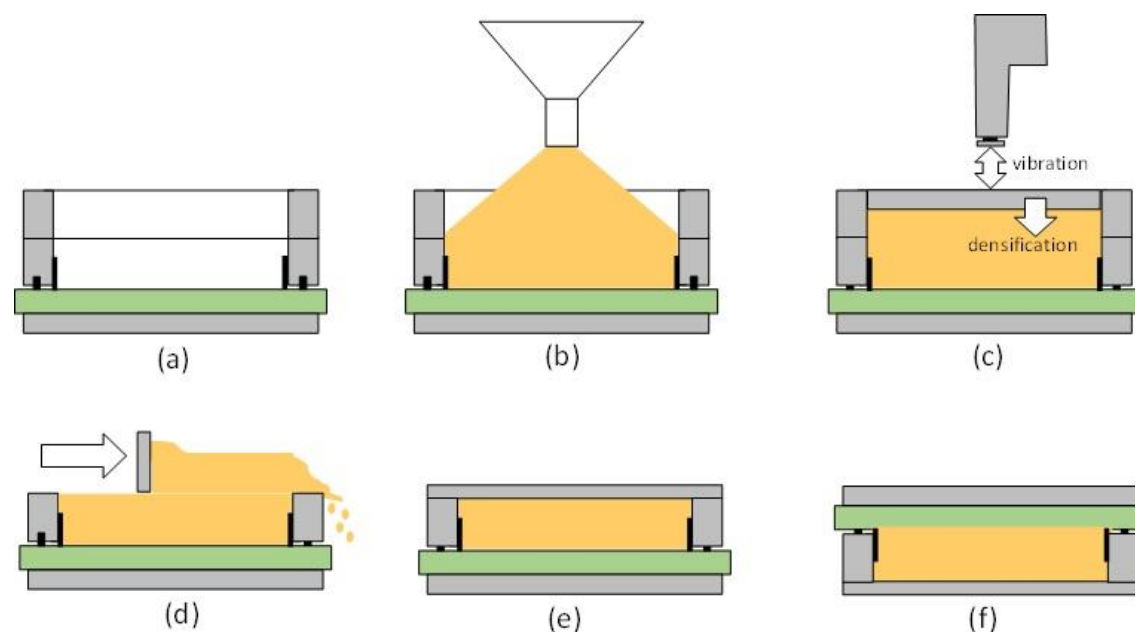


Figure 7 Schematic representation of the step by step procedure for fabrication of interface test samples: (a) securing of the box and addition of an extension; (b) pouring of the material; (c) densification through vibration; (d) removal of excess material; (e) securing of the box; (f) inverting to the upper interface configuration.

5. Testing procedure and program

An initial set of 30 direct shear and 30 interface shear tests were conducted which was later supplemented by an additional set of 10 interface tests investigating the effect of surface seams on shear response. Table 2 and Table 3 detail the main tests and include some key parameters

for direct shear and interface shear tests respectively. The ultimate shear stress, τ_{ult} , is taken as the average shear stress between 10 mm and 12 mm of horizontal displacement, while the peak shear stress, τ_{peak} , is the maximum shear stress recorded during the test. The void ratio of the samples after consolidation by application of the normal load is indicated by e . For each mix, two nominal relative densities were tested (D_r approximately 20% and 70%) at five levels of vertical confining stress, σ_n (approximately 2, 5, 10, 20 and 35 kPa). A four-part test naming convention has been adopted to uniquely identify each test consisting of a soil-type reference [S0, S15, S35], a test type reference [S (for direct shear), I (for interface)], a density reference [L (for loose), D (for dense)], and a stress level reference [2, 5, 10, 20, 35 (kPa)]. The horizontal displacement rate was 0.5 mm/minute.

Table 2 Summary of direct shear tests

| Test name | σ_n (kPa) | Dr_{con} (%) | e_{con} | τ_{peak} (kPa) | τ_{ult} (kPa) | τ_{peak}/σ_n | τ_{ult}/σ_n |
|------------|---------------------|-------------------|-----------|------------------------|-----------------------|------------------------|-----------------------|
| S0_S_L_02 | 2.87 | 21.0 | 0.859 | 1.84 | 1.76 | 0.64 | 0.61 |
| S0_S_L_05 | 5.94 | 14.9 | 0.871 | 3.92 | 3.82 | 0.66 | 0.64 |
| S0_S_L_10 | 11.91 | 30.2 | 0.841 | 8.04 | 7.11 | 0.67 | 0.60 |
| S0_S_L_20 | 22.13 | 14.6 | 0.872 | 14.49 | 13.30 | 0.65 | 0.60 |
| S0_S_L_35 | 37.45 | 28.5 | 0.844 | 24.99 | 23.43 | 0.67 | 0.63 |
| S0_S_D_02 | 2.89 | 69.1 | 0.763 | 3.62 | 2.06 | 1.25 | 0.71 |
| S0_S_D_05 | 5.26 | 74.0 | 0.753 | 5.51 | 3.74 | 1.05 | 0.71 |
| S0_S_D_10 | 11.49 | 73.3 | 0.754 | 9.70 | 7.51 | 0.84 | 0.65 |
| S0_S_D_20 | 22.14 | 73.1 | 0.755 | 17.28 | 13.44 | 0.78 | 0.61 |
| S0_S_D_35 | 37.46 | 84.1 | 0.733 | 29.26 | 23.27 | 0.78 | 0.62 |
| S15_S_L_02 | 2.90 | 21.2 | 0.721 | 2.32 | 2.02 | 0.80 | 0.70 |
| S15_S_L_05 | 5.28 | 27.2 | 0.710 | 3.60 | 3.54 | 0.68 | 0.67 |
| S15_S_L_10 | 11.19 | 18.6 | 0.726 | 7.49 | 7.14 | 0.67 | 0.64 |
| S15_S_L_20 | 22.15 | 9.3 | 0.743 | 15.21 | 15.15 | 0.69 | 0.68 |
| S15_S_L_35 | 37.48 | 11.0 | 0.740 | 24.30 | 23.93 | 0.65 | 0.64 |
| S15_S_D_02 | 2.92 | 73.6 | 0.622 | 3.26 | 2.32 | 1.12 | 0.79 |
| S15_S_D_05 | 5.29 | 63.3 | 0.641 | 5.13 | 4.68 | 0.97 | 0.88 |
| S15_S_D_10 | 11.95 | 70.1 | 0.628 | 10.69 | 8.29 | 0.89 | 0.69 |
| S15_S_D_20 | 22.16 | 76.2 | 0.617 | 18.51 | 14.23 | 0.84 | 0.64 |
| S15_S_D_35 | 37.46 | 73.9 | 0.621 | 30.53 | 24.73 | 0.82 | 0.66 |
| S35_S_L_02 | 2.91 | 3.2 | 0.634 | 2.45 | 2.03 | 0.84 | 0.70 |
| S35_S_L_05 | 5.29 | 0.2 | 0.639 | 3.69 | 3.42 | 0.70 | 0.65 |
| S35_S_L_10 | 11.95 | 15.5 | 0.613 | 8.97 | 8.61 | 0.75 | 0.72 |
| S35_S_L_20 | 22.16 | 3.0 | 0.635 | 14.77 | 14.37 | 0.67 | 0.65 |

| | | | | | | | |
|-------------------|-------|------|-------|-------|-------|------|------|
| S35_S_L_35 | 37.49 | 11.8 | 0.620 | 24.59 | 24.10 | 0.66 | 0.64 |
| S35_S_D_02 | 2.95 | 48.8 | 0.556 | 3.47 | 2.50 | 1.18 | 0.85 |
| S35_S_D_05 | 5.32 | 54.7 | 0.545 | 4.89 | 3.74 | 0.92 | 0.70 |
| S35_S_D_10 | 11.99 | 68.9 | 0.521 | 11.16 | 8.53 | 0.93 | 0.71 |
| S35_S_D_20 | 22.20 | 65.2 | 0.527 | 18.20 | 16.12 | 0.82 | 0.73 |
| S35_S_D_35 | 37.52 | 77.6 | 0.506 | 27.65 | 24.25 | 0.74 | 0.65 |

Table 3 Summary of interface tests

| Test name | σ_n (kPa) | Surface ref. | Mean R_a/D_{50} | Dr_{con} (%) | e_{con} | τ_{peak} (kPa) | τ_{ult} (kPa) | τ_{peak}/σ_n | τ_{ult}/σ_n |
|-------------------|---------------------|-----------------|----------------------|-------------------|-----------|------------------------|-----------------------|------------------------|-----------------------|
| S0_I_L_02 | 2.26 | PP26 | 0.001647 | 17.1 | 0.867 | 0.93 | 0.90 | 0.41 | 0.40 |
| S0_I_L_05 | 5.89 | PP22 | 0.001165 | 23.7 | 0.854 | 2.41 | 2.37 | 0.41 | 0.40 |
| S0_I_L_10 | 12.01 | PP25 | 0.001004 | 19.8 | 0.861 | 4.14 | 4.04 | 0.35 | 0.34 |
| S0_I_L_20 | 22.22 | PP24 | 0.001245 | 11.3 | 0.878 | 8.00 | 7.39 | 0.36 | 0.33 |
| S0_I_L_35 | 37.54 | PP27 | 0.001245 | 10.5 | 0.880 | 14.30 | 13.39 | 0.38 | 0.36 |
| S0_I_D_02 | 2.27 | PP09 | 0.001526 | 77.6 | 0.746 | 1.08 | 1.04 | 0.47 | 0.46 |
| S0_I_D_05 | 5.90 | PP04 | 0.001446 | 80.3 | 0.740 | 3.00 | 2.93 | 0.51 | 0.50 |
| S0_I_D_10 | 12.03 | PP03 | 0.001205 | 74.7 | 0.752 | 5.19 | 4.80 | 0.43 | 0.40 |
| S0_I_D_20 | 22.24 | PP02 | 0.001647 | 73.7 | 0.754 | 8.85 | 8.60 | 0.40 | 0.39 |
| S0_I_D_35 | 37.56 | PP01 | 0.001245 | 69.4 | 0.762 | 14.45 | 12.68 | 0.38 | 0.34 |
| S15_I_L_02 | 2.28 | PP18 | 0.001132 | 14.1 | 0.734 | 0.87 | 0.86 | 0.38 | 0.38 |
| S15_I_L_05 | 5.90 | PP23 | 0.001208 | 32.7 | 0.699 | 2.41 | 2.30 | 0.41 | 0.39 |
| S15_I_L_10 | 12.03 | PP21 | 0.001132 | 28.0 | 0.708 | 4.75 | 4.70 | 0.39 | 0.39 |
| S15_I_L_20 | 22.24 | PP19 | 0.001132 | 14.1 | 0.734 | 7.83 | 7.69 | 0.35 | 0.35 |
| S15_I_L_35 | 37.56 | PP17 | 0.001132 | 15.1 | 0.732 | 12.80 | 12.39 | 0.34 | 0.33 |
| S15_I_D_02 | 2.29 | PP09* | 0.001434 | 74.5 | 0.620 | 1.28 | 1.24 | 0.56 | 0.54 |
| S15_I_D_05 | 5.92 | PP11* | 0.001736 | 82.1 | 0.606 | 3.37 | 3.29 | 0.57 | 0.56 |
| S15_I_D_10 | 12.04 | PP16 | 0.001283 | 74.6 | 0.620 | 4.99 | 4.93 | 0.41 | 0.41 |
| S15_I_D_20 | 22.26 | PP13* | 0.001245 | 75.4 | 0.619 | 11.69 | 11.50 | 0.53 | 0.52 |
| S15_I_D_35 | 37.58 | PP26* | 0.001547 | 69.4 | 0.608 | 16.00 | 14.67 | 0.43 | 0.39 |
| S35_I_L_02 | 2.29 | PP13 | 0.000968 | 25.7 | 0.596 | 0.88 | 0.83 | 0.38 | 0.36 |
| S35_I_L_05 | 5.92 | PP08 | 0.000821 | 33.7 | 0.582 | 2.27 | 2.20 | 0.38 | 0.37 |
| S35_I_L_10 | 12.04 | PP14 | 0.001584 | 21.5 | 0.603 | 4.79 | 4.64 | 0.40 | 0.39 |
| S35_I_L_20 | 22.25 | PP15 | 0.000997 | 23.1 | 0.600 | 8.56 | 7.91 | 0.38 | 0.36 |
| S35_I_L_35 | 37.58 | PP07 | 0.000850 | 31.4 | 0.586 | 13.70 | 13.34 | 0.36 | 0.36 |
| S35_I_D_02 | 2.30 | PP11 | 0.001349 | 64.4 | 0.529 | 1.11 | 1.07 | 0.48 | 0.47 |
| S35_I_D_05 | 5.93 | PP05 | 0.001114 | 82.2 | 0.498 | 3.15 | 3.06 | 0.53 | 0.52 |
| S35_I_D_10 | 12.06 | PP12 | 0.001290 | 73.0 | 0.514 | 5.39 | 5.25 | 0.45 | 0.44 |
| S35_I_D_20 | 22.27 | PP10 | 0.000938 | 69.7 | 0.519 | 9.56 | 8.95 | 0.43 | 0.40 |
| S35_I_D_35 | 37.59 | PP06 | 0.001056 | 76.0 | 0.509 | 16.54 | 16.26 | 0.44 | 0.43 |

Due to a shortfall in the required number of surface specimens, four were subjected to two interface tests. Such tests are denoted by an asterisk () following the surface reference in Column

3. The effect of the former test on subsequent data has been minimised by selecting for retest only those surface specimens that experienced low levels of σ'_n .

Table 4 details the 10 additional tests to investigate the influence of surface seams. These tests utilised the soil S0 in dense condition as indicated by the test name and with additional nomenclature [nS (for no seam), wS (for with seam)].

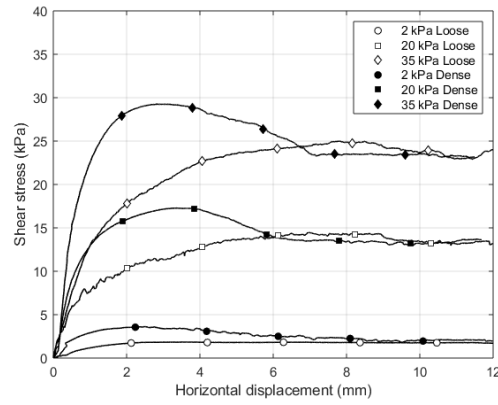
Table 4 Summary of additional interface tests

| Test name | σ_n (kPa) | Surface ref. | Dr_{con} (%) | E_{con} | τ_{peak} (kPa) | τ_{ult} (kPa) | τ_{peak}/σ_n | τ_{ult}/σ_n |
|--------------|---------------------|-----------------|-------------------|-----------|------------------------|-----------------------|------------------------|-----------------------|
| S0_I_D_02_nS | 2.06 | PP28 | 70.1 | 0.760 | 1.00 | 0.99 | 0.49 | 0.48 |
| S0_I_D_05_nS | 5.13 | PP28 | 70.0 | 0.760 | 2.16 | 2.13 | 0.42 | 0.42 |
| S0_I_D_10_nS | 11.26 | PP28 | 70.1 | 0.760 | 4.48 | 4.19 | 0.40 | 0.37 |
| S0_I_D_20_nS | 21.49 | PP28 | 70.1 | 0.760 | 8.36 | 7.84 | 0.39 | 0.36 |
| S0_I_D_35_nS | 36.83 | PP28 | 70.1 | 0.760 | 13.55 | 12.40 | 0.37 | 0.34 |
| S0_I_D_02_wS | 2.06 | PP09 | 63.9 | 0.770 | 1.02 | 1.00 | 0.50 | 0.49 |
| S0_I_D_05_wS | 5.13 | PP09 | 70.1 | 0.760 | 2.16 | 2.12 | 0.42 | 0.41 |
| S0_I_D_10_wS | 11.26 | PP09 | 59.4 | 0.780 | 4.24 | 4.18 | 0.38 | 0.37 |
| S0_I_D_20_wS | 21.49 | PP09 | 70.2 | 0.760 | 8.04 | 7.93 | 0.37 | 0.37 |
| S0_I_D_35_wS | 36.83 | PP09 | 70.1 | 0.760 | 13.62 | 13.29 | 0.37 | 0.36 |

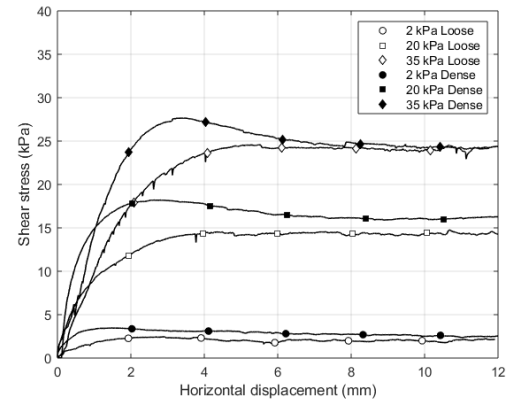
6. Experimental results

6.1 Typical direct and interface shear behaviour

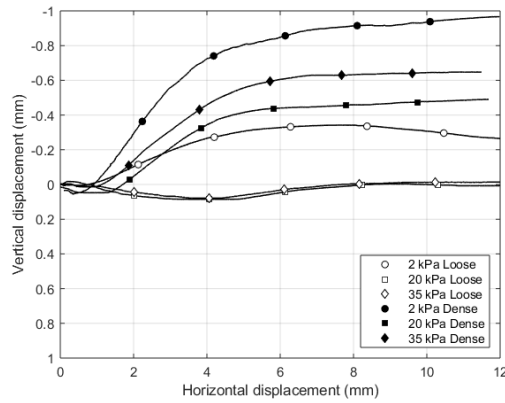
Representative direct shear and interface results are presented in Figure 8 and Figure 9 respectively. For convenience and clarity in the figures, the range of stresses and soil gradings are represented by presenting only the results for soil S0 and S35 at 2, 20, and 35 kPa. For dense sands tested in direct shear, peak strengths are mobilised in the early stages that coincide with maximum rates of dilation. As rates of dilation fall, so does the shear resistance until a near-constant ultimate state is mobilised. Loose samples exhibit a monotonic increase of shear resistance to a near-constant ultimate state accompanied by either no or very limited dilation. The ultimate strength of dense and loose samples falls within a narrow range. The rotation of the top plate was very limited and within 2° of horizontal for all the direct shear tests, which is within the typical range of the winged direct shear apparatus.



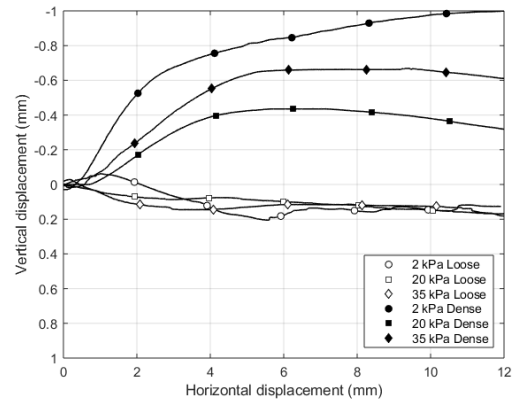
(a) S0 shear stress-horizontal displacement



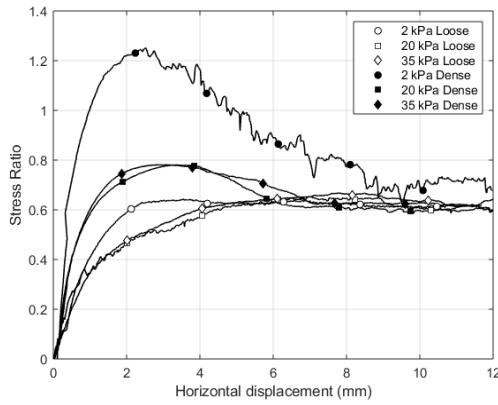
(b) S35 shear stress-horizontal displacement



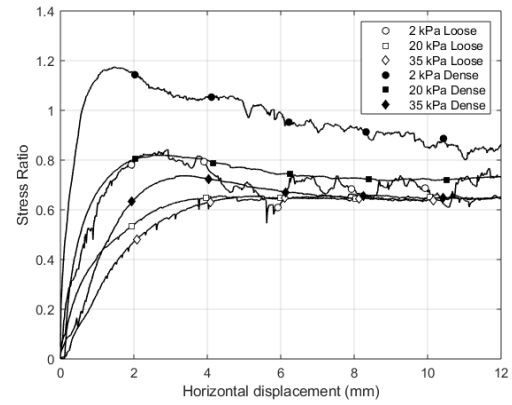
(c) S0 vertical-horizontal displacement



(d) S35 vertical-horizontal displacement



(e) S0 shear to normal stress ratio

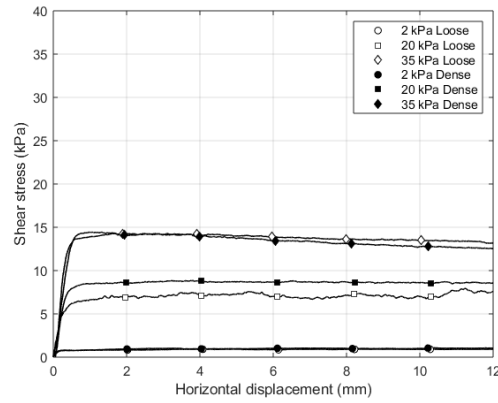


(f) S35 shear to normal stress ratio

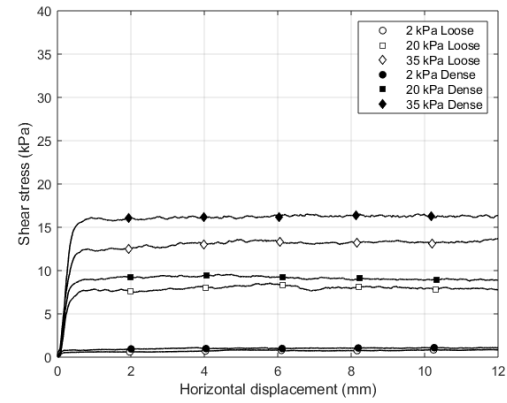
Figure 8 Direct shear soil test results for sand mixtures S0 and S35 for both loose and dense configurations at three stress levels.

237

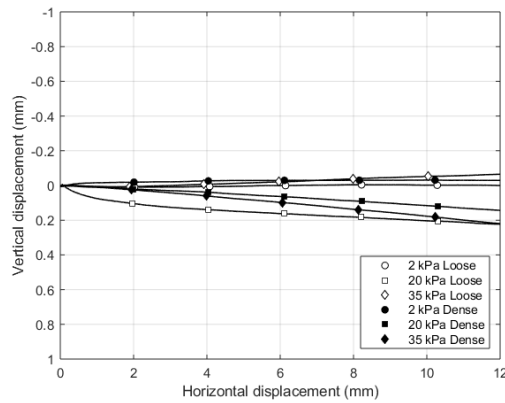
238 For both dense and loose samples, interface tests exhibit a steady increase in shear stress until
 239 a plateau is reached at a horizontal displacement of less than 0.5 mm. From then on, the shear
 240 stress remains nearly constant until the end of the test. Interface shear strengths are lower than
 241 their direct shear counterparts. There is little or no volumetric change during interface tests which
 242 is indicative of a particle sliding kinematic (O'Rourke *et al.*, 1990; Dove and Frost, 1999).



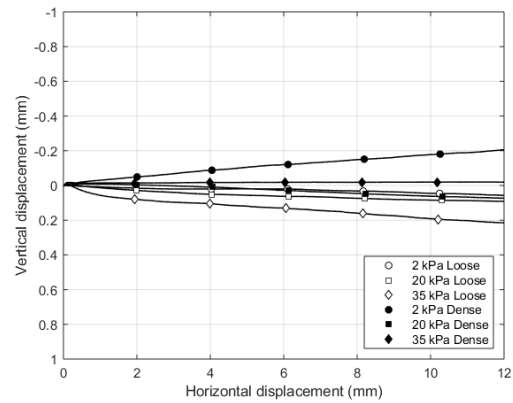
(a) S0 shear stress-horizontal displacement



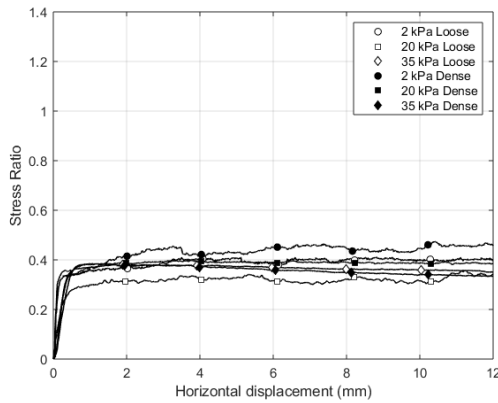
(b) S35 shear stress-horizontal displacement



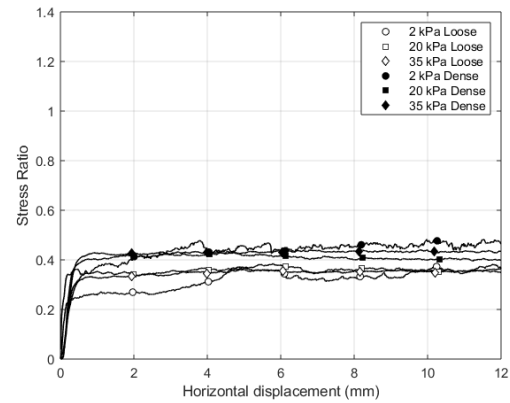
(c) S0 vertical-horizontal displacement



(d) S35 vertical-horizontal displacement



(e) S0 shear to normal stress ratio



(f) S35 shear to normal stress ratio

Figure 9 Interface shear test results for sand mixtures S0 and S35 and polypropylene surface for both loose and dense configurations at three stress levels.

243

244

245

246

247

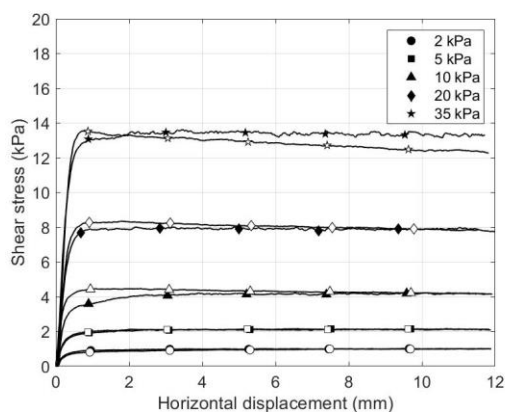
248

For each stress level, the shear stress-displacement response shows a steady increase up to a relatively stable value which increases with the applied normal stress. At the highest normal stress of ~35 kPa, shear stress-displacement behaviour sometimes exhibits a slight initial maximum, and is more visible for dense samples (i.e. Figure 9c). The volumetric trends show a generally flat response, irrespective of the applied normal stress level, with vertical movement of

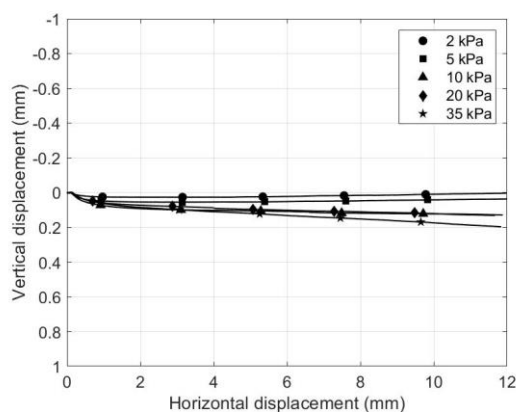
the top pad within 0.2 mm for all the tests supporting the inference of a grain sliding kinematic across all stress levels. For consistency with direct shear, the peak and ultimate state terminology, with the same definition, is used in discussing interface results despite a lack of peak-postpeak behaviour.

6.2 Influence of surface seams

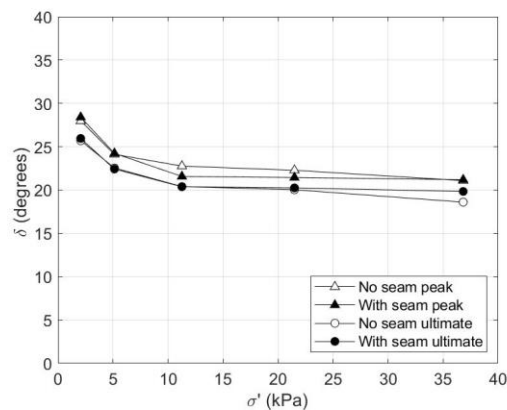
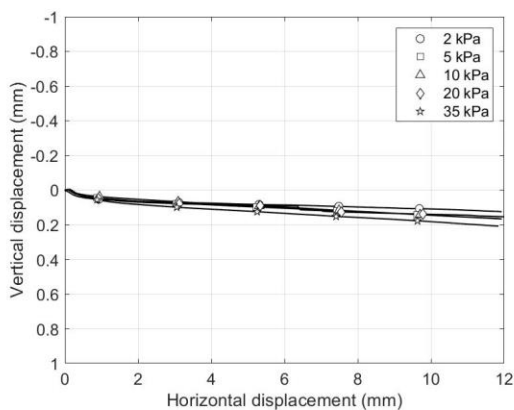
Figure 10 presents the interface test data relating to the influence of surface seams on interface shear response. For both surfaces the response is consistent with the interface shear responses observed in other tests. There is an initial increase in strength which then remains largely stable for the duration of the test. The surface without a seam shows a very subtle tendency to a slight maximum and the vertical displacement trends exhibit a tighter spread than the seamed surface. In both cases, however, there is very little volumetric behaviour, exhibiting only a subtle tendency to contract. Figure 10d shows mobilised peak and ultimate friction angles with stress level. It is concluded that surface seams have little influence on the measured interface shear response.



(a) Stress-horizontal displacement for surfaces with (black) and without (white) seam



(b) Vertical-horizontal displacement for surfaces with a seam



(c) Vertical-horizontal displacement for surfaces without a seam

(d) Friction angles for seamed and unseamed surfaces

Figure 10 S0 (a) shear stress, (b, c) vertical displacement, and (d) peak and ultimate angle of friction for dense tests on counterfaces with and without a seam.

6.3 Influence of coarse fraction content

Peak angle of friction for both soil and interface tests are compared in Figure 11. It should be noted that due to the lack of peak-postpeak behaviour for interface tests, peak angle of friction is analogous to its ultimate strength. Larger friction angle values are observed for higher coarse material content with an increase of about 1.6° , from 31.8° to 33.4° , from S0 to S35 mixtures. The values for interface friction angle exhibit a similar increase with the greater coarse particle content; for both loose and dense configurations an increase of about 1° is apparent.

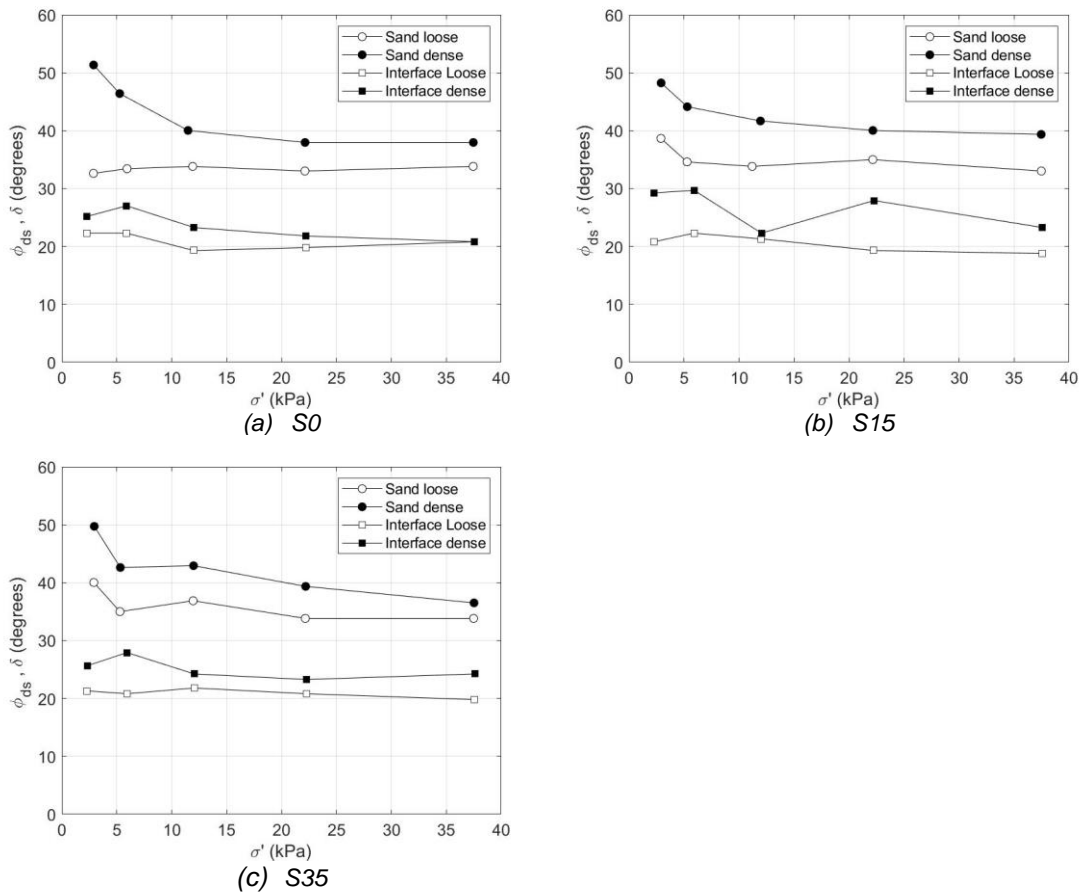


Figure 11 Peak angle of friction and normal stress for direct shear and interface shear tests on (a) S0, (b) S15 and (c) S35 mixtures.

6.4 Influence of stress level

In both soil and interface tests there is a marked nonlinearity in the strength envelopes with lower normal stresses generally presenting enhanced shear strengths, shown in Figure 11. Higher strengths at low stress levels are a common feature of the response of granular geomaterials, e.g. Sture *et al.* (1998), Fannin *et al.* (2005), Chakraborty and Salgado (2010). In interface tests there is a generally tendency for the interface strength to reduce with increasing stress level. Dove and Frost (1999) provided a theoretical explanation for such an increase based on the evolution of the contact area and stress between particles and the counterface, suggesting a power law decrease of interface friction angle with increasing stress level.

6.4 Influence of density

Examination of Figure 11 reveals that there is a notable tendency for dense sample tests to mobilise a greater interface shear strength than loose sample tests. Loose sample tests for S0, S15, and S35 had angles of friction of 19.8°, 20.3°, and 20.3° respectively compared to dense tests which had 22.8°, 25.6°, and 24.2° respectively. The average increase in strength from loose to dense sample tests was approximately 4°. A dependence on density for polypropylene interface strength and a 4° increase in strength for dense sample tests corroborates the findings of O'Rourke *et al.* (1990) but is contrary to the behaviour of metal interfaces (Yoshimi and Kishida, 1981; Noorany, 1985; Jardine *et al.* 1993; Porcino *et al.* 2003). Greater interface strength with higher sample density may be caused by the greater number of particles present at the surface compared to a loose sample (Dove and Frost, 1999). It is conjectured that more particles contacting the surface causes more contact points and generates greater resistance to shearing.

7. Surface topography

To quantify the degree to which the surface topography is modified by processes at the interface, the differences between the pre-test and the post-test parameters (presented in Figure 5) are calculated. Figure 12 presents these deviations against the different test variables: stress level, soil density, and soil mix type. Lines of best fit have been plotted through the data to reveal any underlying trends. Also shown in Figure 12 are the relevant coefficients of variation as dotted lines to represent the variability inherent in the roughness.

Figure 12 reveals that for the considered levels of stress and horizontal displacement at the interface, the effect of interface displacement on surface roughness generally remains within the natural variability in the direction of shear (i.e. in the X direction). Across the direction of shear (i.e. in the Y direction) there is a discernible positive trend between roughness and stress level consistent with the action of sliding a collection of particles across a relatively soft counterface, leaving near-parallel striations in their wake. As the stress level increases, the surface modification becomes more pronounced. Soil density and coarse particle content appear to have little or no influence on the evolution of the surface topography, within the scope of this research.

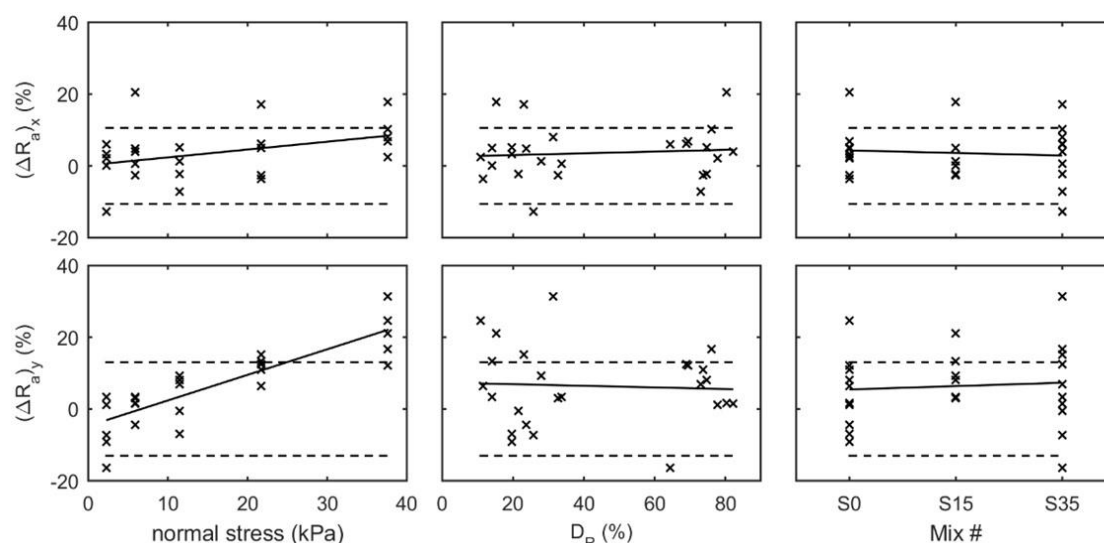


Figure 12 The influence of stress level, relative density and soil type of an interface test on the resultant surface specimen roughness in the X and Y direction.

8. Discussion

8.1 Interface to soil strength ratio

The interface efficiencies, the ratio of interface strength to equivalent soil-only strength, for each surface and sand type are considered and presented in Figure 13. Despite some scatter in the data (especially for lower normal stress levels) the three materials have similar ratios, varying between 0.50 to 0.70 (excluding S15 at ~20 kPa which is an outlier), and may be due to each test soils having the same base sand component.

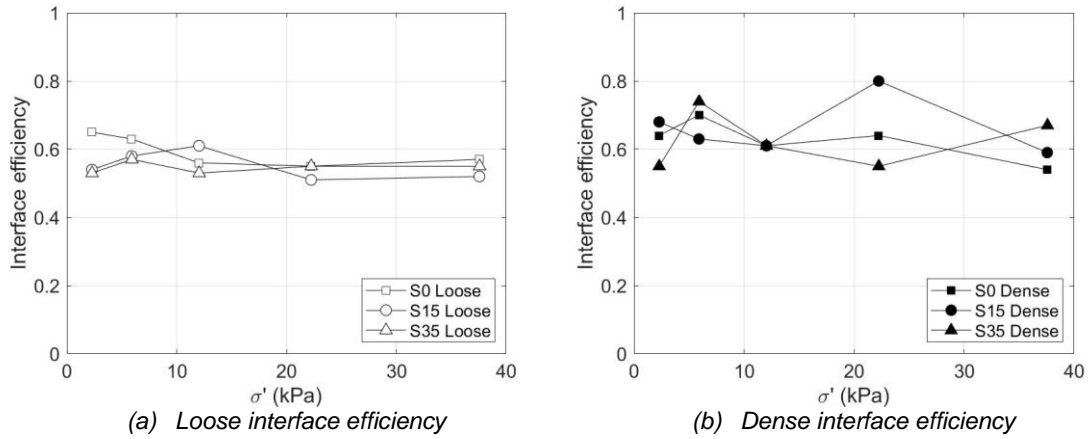


Figure 13 Interface efficiency ratio for loose and dense test configurations.

The averages for each material and density configuration range between 0.55 to 0.62 with maximum standard deviation of 0.05 suggesting that for the three materials an approximated ratio equal to 0.60 (calculated by averaging all the test results) may be assumed. It is important to note that the interface to soil strength ratio is different from the interface friction coefficient. Instead, it is a measure of the interface efficiency which determines how much of the soil strength is mobilised on the interface.

Considering a large range of polymers, O'Rourke *et al.* (1990) showed that a polymer's Shore D hardness has an important role in determining the mechanism of interface shear. The ratio between peak interface shear strength and soil angle of friction decreases with increasing Shore D hardness (Figure 14) as the interaction mechanism progressively evolves from rolling to sliding. Peak polypropylene interface strength from dense sample tests averaged across stress levels of ~10, ~20, and ~35 kPa are presented in Figure 14 and fit the trend proposed by O'Rourke *et al.* (1990) reasonably well. According to the surface topography measurements and the interface test results showing an absence of volumetric deformation, the inferred interaction mechanism is sliding with limited ploughing as suggested by O'Rourke *et al.* (1990) for materials with similar Shore D hardness.

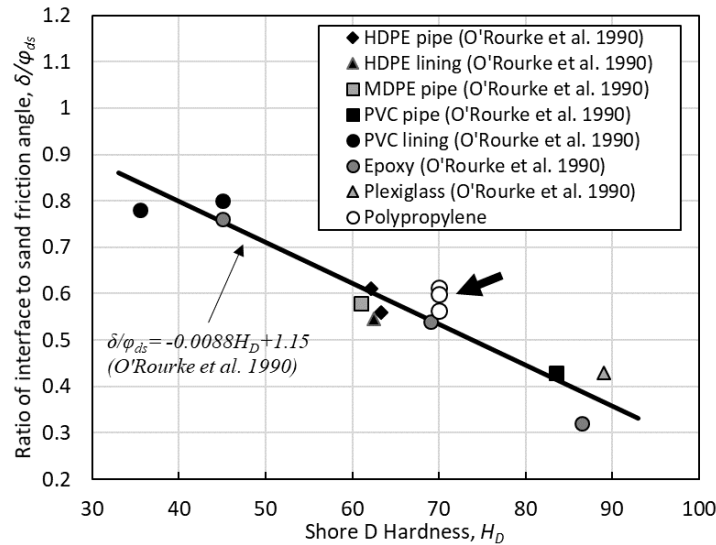


Figure 14 Ratio of peak polymer interface to peak soil friction angle with Shore D hardness at 20.7kPa confining stress after O'Rourke (1990), and peak polypropylene interface strength averaged from data at ~10, ~20, and ~35 kPa confining stress.

8.2 Interface strength and normalised roughness

Interface shear strength is strongly influenced by the roughness of the surface, typically normalised by the grain size using either R_{max}/D_{50} or R_a/D_{50} as suggested by Uesugi and Kishida (1986) and Jardine *et al.* (1993) respectively. Lings and Dietz (2005) demonstrated that for hard counterfaces, such as steel, both expressions of normalised roughness are effective in capturing the evolution of interface strength with roughness. Steel surfaces tend to have generally uniform distributions of roughness and surface texture, particularly those the subject of interface research. However, the polypropylene in this research and in its real-world application may contain individual large-amplitude features such as seams from the manufacturing process, which are not representative of the whole surface. Figure 15 presents the variation of peak shear stress ratio with normalised roughness using (a) R_{max}/D_{50} and (b) R_a/D_{50} for tests conducted at nominal stress levels of ~20 kPa. The average R_a/D_{50} for each test is detailed in Table 3.

Dietz and Lings (2005) identified zones (featured in Figure 15) where surfaces are characterised as smooth or rough, or transitional. In the smooth zone there is little or no volumetric change during shearing which is associated with a lack of dilatant response and a grain sliding kinematic. In the rough zone shearing is fully dilatant and volumetric responses are observed consistent with stress-dilatancy. Between the smooth and rough zone is a transition where increasing levels of

dilatancy occur until fully dilatant responses are observed. Using R_{max} as in Figure 15a suggests there ought to be a degree of dilatancy during shearing with associated peak-postpeak behaviour but this is not reflected in the data. Use of R_a in Figure 15b suggests little or no dilatancy which is consistent with the behaviour seen in the present data for polypropylene.

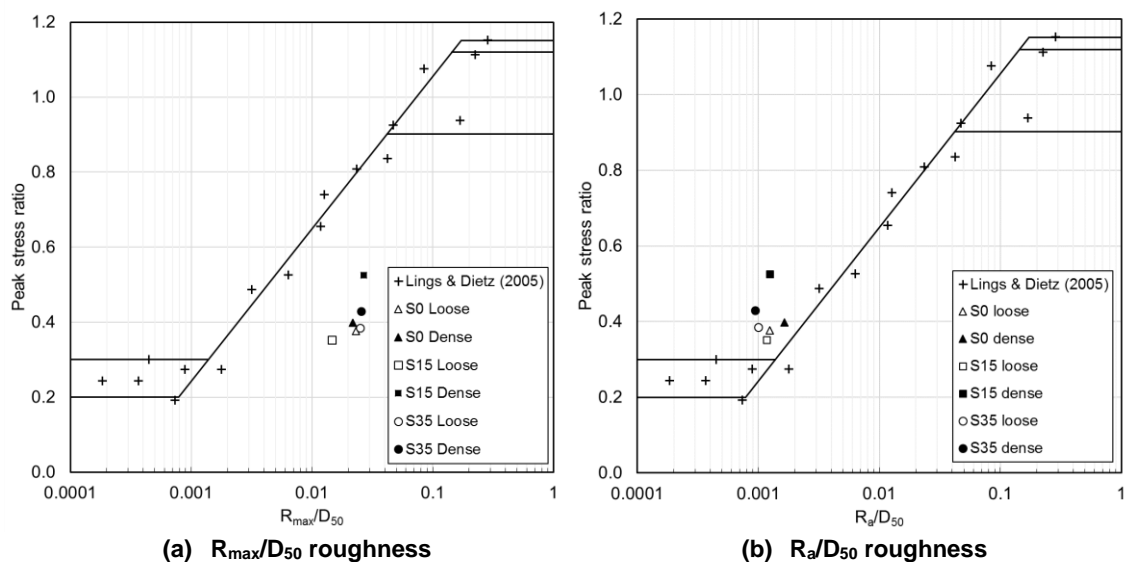


Figure 15 Peak shear stress to normal stress ratio with (a) R_a/D_{50} and (b) R_{max}/D_{50} with data for coarse, medium, and fine sand and trend lines for sand-steel interface after Lings and Dietz (2005).

It has been shown already that the presence of a single seam across surfaces does not affect the interface shear strength. It has also been shown that R_a is the more appropriate metric of surface roughness as it agrees better with the stress and volumetric responses seen in the data. Therefore, if there are unique large amplitude features present which are not representative of the whole surface, R_a is the preferable method of quantifying surface roughness.

Adopting R_a as in Figure 15b to characterise the relationship between interface strength and roughness, it is apparent that for equivalent magnitudes of roughness, polypropylene surfaces offer an enhanced interface strength over steel surfaces. The greater strength may be explained by an extension of O'Rourke's (1990) observation about hardness and strength to include steel-surfaces. Polypropylene is less hard than steel, therefore, a greater shear strength is mobilised.

9. Conclusions

The results of an experimental program investigating the interface shear behaviour of sand-polypropylene pipeline coating specimens at low stress levels have been presented. The test soils were prepared to represent typical sediments of the North Sea basin and the influence of varying amounts of coarse particles fraction has been investigated. Some clear trends and information about the soil-surface interaction mechanism are evident:

- Polypropylene interface tests generally exhibit an elastic, perfectly plastic type response for both loose and dense samples, where the shear stress increases to a plateau during the early stages and then remains largely stable throughout the duration of the test.
- Interface shear stresses are enhanced at very low stresses creating non-linear failure envelopes consistent with established behaviours for soil friction.
- Contrary to soil friction behaviour, there is a modest enhancement in shear strength observed in dense interface tests over loose suggesting it is a characteristic of polymer interfaces in general and not due solely to interface test configuration.
- Surface specimens which had a seam running across the face did not exhibit behaviour significantly different from those without, and there was no distinct increase in strength associated with the presence of the seam.
- Where surfaces are inscribed by distinct extreme features not representative of the whole surface, averaged roughness provides a much more appropriate quantifier than taking the extreme values.
- Damage characteristics and lack of dilatancy during shearing are consistent with a particle sliding kinematic. Sample relative density and coarse fraction content of the tested soils do not have any significant effect on surface roughness that is greater than the natural variability across the specimen set. There appears to be a tendency for higher stress levels to cause greater damage when measured perpendicular to shearing, consistent with formation of surface damage striations parallel to shear direction.
- Friction coefficients ranged between 0.33 and 0.57 across the range of tested interfaces and interface efficiencies were found to range between 0.50 and 0.80 with an average value of approximately 0.6. Friction coefficient varies with stress level, density, and soil coarse fraction content but the interface efficiency seems to be largely independent of these variables.

403

404 **Acknowledgements**

405 The authors wish to thank TechnipFMC for commissioning and specifying the scope of this
406 research and acknowledge the technical collaboration on this project.

407

408 **References**

409 Al-Douri, R.H., Poulos, H.G. 1992. Static and cyclic direct shear tests on carbonate sands.
410 *Geotechnical Testing Journal*, 15 (2), pp.138-157.

411 Bruton, D.A.S., White, D.J., Cheuk, J.C.Y. 2008. Pipe-soil interaction during lateral buckling and
412 pipeline walking – the SAFEBUCK JIP. In: *Proceedings of the Offshore Technology*
413 *Conference*, Houston, Texas, USA.

414 BS1377-2:1990. Methods of test for soils for civil engineering purposes - part 2: classification
415 tests. *British Standards Institute*, London, United Kingdom.

416 BS1377-4:1990. Methods of test for soils for civil engineering purposes - part 4: compaction
417 related tests. *British Standards Institute*, London, United Kingdom.

418 Carr, M., Bruton, D., Leslie, D. 2003. Lateral buckling and pipeline walking, a challenge for hot
419 pipelines. In: *Proceedings of the Offshore Pipeline Technology Conference*, Amsterdam, The
420 Netherlands, pp.1-36.

421 Cathie, D.N., Jaek, C., Ballard, J.C., Wintgens, J.F. 2005. Pipeline geotechnics – state-of-the-
422 art. In: *Proceedings of the International Symposium on the Frontiers in Offshore Geotechnics*,
423 Perth, Australia, pp.95-114.

424 Chakraborty, T., Salgado, R., 2010. Dilatancy and shear strength of sand at low confining
425 pressures. *Journal of Geotechnical and Geoenvironmental Engineering*, 136 (3), pp. 527-532.

426 De Leeuw, L.W., Diambra, A., Dietz, M.S., Mylonakis, G., Milewski, H. 2019. Interface shear
427 strength of polypropylene pipeline coatings and granular materials at low stress level. *E3S*
428 *Web of Conferences*, 92, pp.13010.

429 Dietz, M.S., Lings, M.L. 2006. Postpeak strength of interfaces in a stress-dilatancy framework.
430 *Journal of Geotechnical and Geoenvironmental Engineering*, 132 (11), pp. 1474-1484.

431 DNVGL, 2017a. On-bottom stability design of submarine pipelines, DNVGL-RP-F109. Oslo,
432 Norway.

433 DNVGL, 2017b. Pipe-soil interaction for submarine pipelines, DNVGL-RP-F114. Oslo, Norway.

434 Dove, J.E., Frost, J.D. 1999. Peak friction behavior of smooth geomembrane-particle interfaces.

435 *Journal of Geotechnical and Geoenvironmental Engineering*, 125 (7), pp. 544-555.

436 Fannin, R.J., Eliadorani, A., Wilkinson, J.M.T. 2005. Shear strength of cohesionless soils at low

437 stress. *Géotechnique*, 55 (6), pp. 467-478.

438 Han, F., Ganju, E., Salgado, R., Prezzi, M. 2018. Effects of Interface Roughness, Particle

439 Geometry, and Gradation on the Sand–Steel Interface Friction Angle. *Journal of Geotechnical*

440 *and Geoenvironmental Engineering*, 144 (12).

441 Hobbs, R.E. 1984. In-service buckling of heated pipelines. *Journal of Transport Engineering*, 110

442 (2), pp.175-189.

443 Ibraim, E., Fourmont, S. 2007. Behaviour of sand reinforced with fibres. In: *Soil stress-strain*

444 *behaviour: Measurement, modelling and analysis*, pp. 807-818. Springer, Dordrecht.

445 Ingold, T.S., 1982. *Reinforced earth*. Eds: Thomas Telford, London

446 Jardine, R.J., Lehane, B.M., Everton, S.J. 1993. Friction coefficients for piles in sands and silts.

447 In: *Offshore Site Investigation and Foundation Behaviour* (pp. 661-677). Springer, Dordrecht.

448 Jewell, R.A., Wroth, C.P. 1987. Direct shear tests on reinforced sand. *Géotechnique*, 37 (1), pp.

449 53-68.

450 Lings, M.L., Dietz, M.S. 2004. An improved direct shear apparatus for sand. *Géotechnique*, 54

451 (4), pp. 245-256.

452 Lings, M.L., Dietz, M.S. 2005. The peak strength of sand-steel interfaces and the role of dilation.

453 *Soils and Foundations*, 45 (6), pp. 1-14.

454 Milewski, H., Dietz, M., Diambra, A., de Leeuw, L.W. 2019. Axial resistance of smooth polymer

455 pipelines on sand. In: *Proceedings of the ASME 2019 38th International Conference on Ocean,*

456 *Offshore and Arctic Engineering*, Glasgow, United Kingdom (*In press*).

457 Miura, K., Maeda, K., Toki, S. 1997. Method of measurement for the angle of repose of sands.

458 *Soils and Foundations*, 37 (2), pp. 89-96.

459 Negussey, D., Wijewickreme, W.K.D., Vaid, Y.P. 1989. Geomembrane interface friction.

460 *Canadian Geotechnical Journal*, 26 (1), pp.165-169.

461 Noorany, I. 1985. Side friction of piles in calcareous sands. In: *Proceedings of the 11th*
462 *International Conference on Soil Mechanics and Foundation Engineering*, San Francisco,
463 USA, pp. 1611-1614.

464 O'Rourke, T.D., Druschel, S.J., Netravali, A.N. 1990. Shear strength characteristics of sand-
465 polymer interfaces. *Journal of Geotechnical Engineering*, 116 (3), pp.451-469.

466 Perinet, D. Simon, J. 2011. Lateral buckling and pipeline walking mitigation in deep water. In:
467 *Proceedings of the Offshore Technology Conference*, Houston, Texas, USA.

468 Porcino, D., Fioravante, V., Ghionna, V. N., Pedroni, S. 2003. Interface behaviour of sands from
469 constant normal stiffness direct shear tests. *Geotechnical Testing Journal*, 26 (3), pp. 289-
470 301.

471 Saxena, S.K., Wong, Y.T. 1984. Friction characteristics of a geomembrane. In *Proceedings of the*
472 *International Conference on Geomembranes* (pp. 187-190).

473 Shibuya, S., Mitachi, T., Tamate, S. 1997. Interpretation of direct shear box testing of sands as
474 quasi-simple shear. *Géotechnique*, 47 (4), pp.769-790.

475 Sture, S., Costes, N.C., Batiste, S.N., Lankton, M.R., AlShibli, K.A., Jeremic, B., Swanson, R.A.,
476 Frank, M. 1998. Mechanics of granular materials at low effective stresses. *Journal of*
477 *Aerospace Engineering*, 11 (3), pp. 67-72.

478 Subba Rao, K.S., Allam, M.M. Robinson, R.G. 1998. Interfacial friction between sands and solid
479 surfaces. *Proceedings of the Institution of Civil Engineering: Geotechnical Engineering*, 131,
480 pp. 75-82.

481 Tornes, K., Jury, J., Ose, B.A., Thompson, P. 2000. Axial creeping of high temperature flowlines
482 caused by soil ratcheting. In: *Proceedings of the 19th International Conference on Offshore*
483 *Mechanics and Arctic Engineering*, New Orleans, Louisiana, USA.

484 Uesugi, M., Kishida, H. 1986. Influential factors of friction between steel and dry sands. *Soils and*
485 *Foundations*, 26 (2), pp. 33-46.

486 Verley, R.L.P., Sotberg, T. 1994. A soil resistance model for pipelines placed on sandy soils.
487 *Journal of Offshore Mechanics and Arctic Engineering*, 116 (3), pp. 145-153.

488 White, D.J., Cathie, D.N. 2011. Geotechnics for subsea pipelines. In *Proceedings of the 2nd*
489 *International Symposium on Frontiers in Offshore Geotechnics*. Perth, Australia (pp. 87-123).

490 Yoshimi, Y., Kishida, T. 1981. A ring torsion apparatus for evaluating friction between soil and
491 metal surfaces. *Geotechnical Testing Journal*, 4 (4), pp. 145-152.